

---

# LEARNING A SUBSPACE OF POLICIES FOR ONLINE ADAPTATION IN REINFORCEMENT LEARNING

Jean-Baptiste Gaya<sup>\*†</sup>  
jbgaya@fb.com

Laure Soulier<sup>†</sup>  
laure.soulier@lip6.fr

Ludovic Denoyer<sup>\*</sup>  
denoyer@fb.com

## ABSTRACT

Deep Reinforcement Learning (RL) is mainly studied in a setting where the training and the testing environments are similar. But in many practical applications, these environments may differ. For instance, in control systems, the robot(s) on which a policy is learned might differ from the robot(s) on which a policy will run. It can be caused by different internal factors (e.g., calibration issues, system attrition, defective modules) or also by external changes (e.g., weather conditions). There is a need to develop RL methods that generalize well to variations of the training conditions. In this article, we consider the simplest yet hard to tackle generalization setting where the test environment is unknown at train time, forcing the agent to adapt to the system’s new dynamics. This online adaptation process can be computationally expensive (e.g., fine-tuning) and cannot rely on meta-RL techniques since there is just a single train environment. To do so, we propose an approach where we learn a subspace of policies within the parameter space. This subspace contains an infinite number of policies that are trained to solve the training environment while having different parameter values. As a consequence, two policies in that subspace process information differently and exhibit different behaviors when facing variations of the train environment. Our experiments carried out over a large variety of benchmarks compare our approach with baselines, including diversity-based methods. In comparison, our approach is simple to tune, does not need any extra component (e.g., discriminator) and learns policies able to gather a high reward on unseen environments.

## 1 INTRODUCTION

In recent years, Deep Reinforcement Learning (RL) has succeeded at solving complex tasks, from defeating humans in board games (Silver et al., 2017) to complex control problems (Peng et al., 2017; Schulman et al., 2017). It relies on different learning algorithms (e.g., A2C - (Mnih et al., 2016), PPO - (Schulman et al., 2017)). These methods aim at discovering a policy that maximizes the expected (discounted) cumulative reward received by an agent given a particular environment. If existing techniques work quite well in the classical setting, considering that the environment at train time and the environment at test time are similar is unrealistic in many practical applications. As an example, when learning to drive a car, a student learns to drive using a particular car, and under specific weather conditions. But at test time, we expect the driver to be able to generalize to any new car, new roads, and new weather conditions. It is critical to consider the generalization issue where one of the challenges is to learn a policy that generalizes and adapts itself to **unseen environments**.

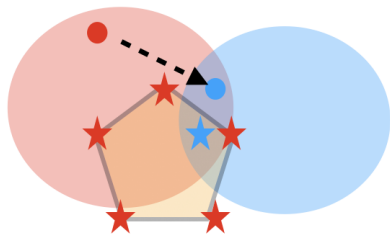
Different techniques have been proposed in the literature (Section 5) to automatically adapt the learned policy to the test environment. In the very large majority of works, the model has access to multiple training environments (meta-RL setting). Therefore, the training algorithm can identify which variations (or invariants) may occur at test time and how to adapt quickly to similar variations. But this setting may still be unrealistic for concrete applications: for instance, it supposes that the student will learn to drive on multiple cars before getting their driving license.

In this paper, we address a simpler yet harder to tackle generalization setting in which the learning algorithm is trained over one single environment and has to perform well on test environments;

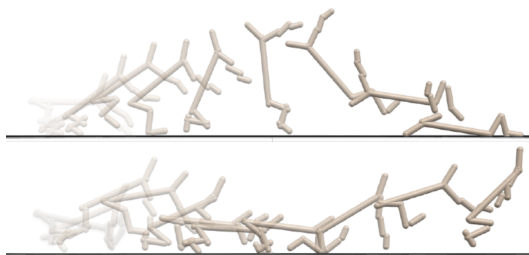
---

<sup>\*</sup>Facebook AI Research

<sup>†</sup>LIP6, Sorbonne Université, France



(a) The figure represents the parameter space. The red (resp. blue) region is the space of good policies over the training (resp. testing) environment. A single learned policy (red point) may be inefficient for the test environment and has to be adapted (e.g., fine-tuning) to become good at test-time (blue point). Instead of learning a single policy, we learn a convex sub-space (the pentagon) delimited by anchor policies (red stars) that aims at capturing a large set of good policies. Then the adaptation is just made by sampling policies in this sub-space, keeping the best one (blue star).



(b) Snapshot of a trajectory on a modified HalfCheetah environment (friction increased by 50%). On top, PPO fails to generalize. On the bottom, our model LoP adapts quickly and finds an efficient policy after a few shot trials.

Figure 1: (Left) An illustration of the process of learning a subspace of policies. (Right) Comparison between PPO and our model in a test environment.

preventing us from using meta-RL approaches. A natural way to attack this setting is to start by learning a single policy using any RL algorithm, and to fine-tune this training policy at test time, over the test environment (See red/blue points in Figure 1a), but this process may be costly in terms of environment interactions.

Very recently, the idea of learning a set of diverse yet effective policies (Kumar et al., 2020b; Osa et al., 2021) has emerged as a way to deal with this adaptation setting. The intuition is that, if instead of learning one single policy, one learns a set of ‘diverse’ policies, then there is a chance that at least one of these policies will perform well over a new dynamics. The adaptation in that case just consists in selecting the best policy in that set by evaluating each policy over few episodes (K-shot adaptation). But the way this set of policies is built and the notion of diversity proposed in these methods have a few drawbacks: these models increase diversity by using an additional intrinsic reward which encourages the different policies to generate different distributions of states. This objective potentially favors the learning of policies that are sub-optimal at train time. Moreover, these approaches make use of an additional component in the policy architecture (e.g., a discriminator) that may be difficult to tune, particularly considering that, at train time, we do not have access to any test environment and thus cannot rely on validation techniques to tune the extra architecture.

Inspired by recent research on mode connectivity (Benton et al., 2021; Kudithipudi et al., 2019) and by (Wortsman et al., 2021) which aims to learn a subspace of models in the supervised learning setting, we propose to learn a **subspace of policies** in the parameter space as a solution to the online adaptation in the RL setting (see Figure 1a). Each particular point in this subspace corresponds to specific parameter values, and thus to a particular policy. This subspace is learned by adapting a classical RL algorithm (PPO and A2C in our case, see Section 3.3) such that an infinite continuum of policies is learned, each policy having different parameters. The policies thus capture and process information differently, and react differently to variations of the training environment (see Figure 1b). We validate our approach (Section 4) over a large set of reinforcement learning environments and compare it with other existing approaches. These experiments show that our method is competitive, achieves good results and does not require the use of any additional component of hyper-parameters tuning contrarily to baselines.

## 2 SETTING

**Reinforcement Learning:** Let us define a state space  $\mathcal{S}$  and an action space  $\mathcal{A}$ . In the RL setting, one has access to a training *Markov Decision Process* (MDP) denoted  $\mathcal{M}$  defined by a transition

distribution  $P(s'|s, a) : \mathcal{S} \times \mathcal{A} \times \mathcal{S} \rightarrow \mathbb{R}_+$ , an initial state distribution  $P^{(i)}(s) : \mathcal{S} \rightarrow \mathbb{R}_+$  and a reward function  $r(s, a) : \mathcal{S} \times \mathcal{A} \rightarrow \mathbb{R}_+$ .

A policy is defined as  $\pi_\theta(a|s) : \mathcal{S} \times \mathcal{A} \rightarrow \mathbb{R}_+$ , where  $\theta$  denotes the parameters of the policy. A trajectory sampled by a policy  $\pi_\theta$  given a MDP  $\mathcal{M}$  is denoted  $\tau \sim \pi_\theta(\mathcal{M})$ . The objective of an RL algorithm is to find a policy that maximizes the expected cumulative (discounted) reward:

$$\theta^* = \arg \max_{\theta} \mathbb{E}_{\tau \sim \pi_\theta(\mathcal{M})} [R(\tau)]$$

where  $R(\tau)$  is the discounted cumulative reward over trajectory  $\tau$ .

**Online adaptation:** We consider the setting where the policy trained over  $\mathcal{M}$  will be used over another MDP (denoted  $\bar{\mathcal{M}}$ ) that shares the same state and action space as  $\mathcal{M}$ , but with a different dynamics and/or initial state distribution and/or reward function<sup>1</sup>. Importantly,  $\bar{\mathcal{M}}$  is unknown at train time, and cannot be used for model selection, making the tuning of hyper-parameters difficult.

Given a trained model, we consider the K-shot adaptation setting where the test phase is decomposed into two stages: a first phase in which the model adapts itself to the new test environment over  $K$  episodes, and a second phase in which the adapted model is used to collect the reward. We thus expect the first phase to be as short as possible (few episodes), corresponding to a fast adaptation to the new environment. Let us consider that a model  $\pi_\theta$  generates a sequence of trajectories  $\bar{\tau}_1, \bar{\tau}_2, \dots, \bar{\tau}_{+\infty}$  over  $\bar{\mathcal{M}}$ , the performance of such a model, is defined as:

$$Perf(\pi_\theta, \bar{\mathcal{M}}, K) = \sum_{t=K+1}^{+\infty} R(\bar{\tau}_t) \quad (1)$$

which corresponds to the performance of the policy  $\pi_\theta$  over  $\bar{\mathcal{M}}$  after  $K$  episodes used for adapting the policy. Note that we are interested in methods that adapt quickly to new a test environment and we will consider small values of  $K$  in our experiments. In the following, for sake of simplicity,  $K$  will refer to the number of policies evaluated during adaptation since each policy may be evaluated over more than a single episode when facing stochastic environments.

### 3 LEARNING SUBSPACES OF POLICIES

**Motivation and Idea:** To illustrate our idea, let us consider a toy example where the train environment contains states with correlated and redundant features, in such a way that multiple subsets of state features can be used to compute good actions to execute. Traditional RL algorithms will discover one policy  $\pi_{\theta^*}$  that is optimal w.r.t the environment. This policy will typically use the state features in a particular way to decide the optimal action at each step. If some features become noisy (at test time) while, unluckily,  $\pi_{\theta^*}$  particularly relies on these noisy features, the performance of the policy will drastically drop. Now, let us consider that, instead of learning just one optimal policy, we also learn a second optimal policy  $\pi_{\theta^{*'}}$ , but enforcing  $\theta^{*'}$  to be different than  $\theta^*$ . This second policy may tend to make use of various features to compute actions. We thus obtain two policies instead of one, and we have more chances that at least one of these policies is efficient at test time. Identifying which of these two policies is the best for the test environment (i.e., adaptation) can simply be done by evaluating each policy over few episodes, keeping the best one. The model we present is built on top of this intuition, extending this example to an infinite set of policies and to variable environment dynamics.

Inspired by Wortsman et al. (2021) which propose to learn a subspace of models for supervised learning, we study the approach of **learning a subspace of policies in the parameter space**, and the use of such a model for online adaptation in reinforcement learning. Studying the structure of the parameter space has seen a recent surge of interest through the *mode connectivity* concept (Benton et al., 2021; Kuditipudi et al., 2019; Wortsman et al., 2021) and obtain good results in generalization, but it has never been involved in the RL setting. As intuitively illustrated in the previous paragraph, we expect that, given a variation of the training environment, having access to a subspace of policies that process information differently instead of a single policy will facilitate the adaptation. As a

<sup>1</sup>In the experimental study, one training environment is associated to multiple test environments to analyze the ability to adapt to different variations.

result, our method is very simple, does not need any extra hyper-parameter to tune and achieve good performance.

### 3.1 SUBSPACES OF POLICIES

Given  $\Theta$  the space of all possible parameters, a subspace of policies is a subset  $\bar{\Theta} \subset \Theta$  that defines a set of corresponding policies  $\bar{\Pi} = \{\pi_\theta\}_{\theta \in \bar{\Theta}}$ .

Since our objective is to learn such a subspace, we have to rely on a parametric definition of such a subspace and consider  $\bar{\Theta}$  as a simplex in  $\Theta$ . Let us define  $N$  anchor parameter values  $\bar{\theta}_1, \dots, \bar{\theta}_N \in \Theta$ . We define the  $\mathcal{Z}$ -space as the set of possible weighted sum of the anchor parameters:  $\mathcal{Z} = \{z = (z_1, \dots, z_N) \in [0, 1]^N \mid \sum z_i = 1\}$ . The subspace we aim to learn is defined by:

$$\bar{\Theta} = \left\{ \sum_{k=1}^N z_k \bar{\theta}_k, \forall z \in \mathcal{Z} \right\} \quad (2)$$

In other words, we aim to learn a convex hull of  $N$  vertices in  $\Theta$ . Note that policies in this subspace can be obtained by sampling  $z \sim p(z)$  uniformly over  $\mathcal{Z}$ .

The advantages of this approach are: a) the number of parameters of the model can be controlled by choosing the number  $N$  of anchor parameters, b) since policies are sharing parameters (instead of learning a set of independent policies), we can expect that the learning will be sample efficient.

Such a subspace is illustrated in Figure 1a through the pentagon (i.e.,  $N = 5$ ) in which angles correspond to the anchor parameters and the surface corresponds to all the policies in the built subspace.

**K-shot adaptation:** Given a subspace of policies  $\bar{\Theta}$ , different methods can be achieved to find the best policy over the test environment. For instance, it could be done by optimizing the distribution  $p(z)$  at test time. In this article, we use the same yet effective K-shot adaptation technique than Kumar et al. (2020b) and Osa et al. (2021): we sample  $K$  episodes using different policies defined by different values of  $z$  that are uniformly spread over  $\mathcal{Z}$ . In our example, it means that we evaluate policies uniformly distributed within the pentagon to identify a good test policy (blue star). Note that, when the environment is deterministic, only one episode per value of  $z$  needs to be executed to find the best policy, which leads to a very fast adaptation.

### 3.2 LEARNING ALGORITHM

Learning a subspace of policies can be done by considering the RL learning problem as maximizing:

$$\mathcal{L}(\bar{\Theta}) = \int_{\theta \in \bar{\Theta}} \mathbb{E}_{\tau \sim \pi_\theta} [R(\tau)] d\theta \quad (3)$$

Considering that  $\bar{\Theta}$  is a convex hull as defined in Equation 2, and using the uniform distribution  $p(z)$  over  $\mathcal{Z}$ , the loss function of Equation 3 can be rewritten as:

$$\mathcal{L}(\bar{\theta}_1, \dots, \bar{\theta}_N) = \mathbb{E}_{z \sim p(z)} [\mathbb{E}_{\tau \sim \pi_\theta} [R(\tau)]] \quad \text{with } \theta = \sum_{k=1}^N z_k \bar{\theta}_k \quad (4)$$

Maximizing such an objective function over  $\bar{\theta}_1, \dots, \bar{\theta}_N$  outputs a (uniform) distribution of policies trained to maximize the reward, all these policies sharing common parameters.

**Avoiding subspace collapse:** One possible effect when optimizing  $\mathcal{L}(\bar{\theta}_1, \dots, \bar{\theta}_N)$  is to reach a solution where all  $\theta_k$  values are similar. In that case, all the policies would have the same parameters value, and will thus all achieve the same performance at test-time. Since we want to encourage the policies to process information differently, and following Wortsman et al. (2021), we encourage the anchor policies to have different parameters. This is implemented through the use of a regularization

term denoted  $C(\bar{\theta}_1, \dots, \bar{\theta}_N)$  that measures how much anchor policies are similar in the parameter space. This auxiliary loss is defined as a pairwise loss between pairs of anchor parameters:

$$C(\bar{\theta}_1, \dots, \bar{\theta}_N) = \sum_{i \neq j} \text{cosine}^2(\theta_i, \theta_j) \quad (5)$$

The final optimization loss is then:

$$\mathcal{L}(\bar{\theta}_1, \dots, \bar{\theta}_N) = \mathbb{E}_{z \sim p(z)} [\mathbb{E}_{\tau \sim \pi_\theta} [R(\tau)]] - \beta \sum_{i \neq j} \text{cosine}^2(\bar{\theta}_i, \bar{\theta}_j) \text{ with } \theta = \sum_{k=1}^N z_k \bar{\theta}_k$$

where  $\beta$  is an hyper-parameter (see Section 4.1 for a discussion) that weights the auxiliary term.

One good property of this loss (in comparison to a method introducing an intrinsic reward) is that this loss does not modify the reward objective of the learned policies and thus does not encourage the model to learn policies that are sub-optimal at train time. In Section 4.1, we show that adding this auxiliary loss does not modify the performance of the model over the training environment, and does not need to be balanced by using any additional hyper-parameters.

Note that the models proposed in (Osa et al., 2021; Kumar et al., 2020b) shares some similarities with our approach with two differences: i) the auxiliary loss is based on an additional neural network used to enforce diversity in the behaviour of the policies. Moreover, in (Kumar et al., 2020b), this term is integrated to the reward while in (Osa et al., 2021), the auxiliary loss can be used only with continuous actions.

### 3.3 LINE OF POLICIES (LOP)

In the case of  $N = 2$ , the subspace of policies corresponds to a simple segment in the parameter space defined by  $\bar{\theta}_1$  and  $\bar{\theta}_2$  as extremities.  $\bar{\theta}_1$  and  $\bar{\theta}_2$  are combined through a single scalar value  $z \in [0; 1]$  as follows:

$$\theta = z\bar{\theta}_1 + (1 - z)\bar{\theta}_2 \quad (6)$$

Computationally, learning a line of policies<sup>2</sup> is similar to learning a single policy for which the number of parameters is doubled, making this particular case a good trade-off between expressivity and training speed. It corresponds to the following objective function:

$$\mathcal{L}(\bar{\theta}_1, \bar{\theta}_2) = \mathbb{E}_{z \sim \mathcal{U}[0;1]} \left[ \mathbb{E}_{\tau \sim \pi_{z\bar{\theta}_1 + (1-z)\bar{\theta}_2}} [R(\tau)] \right] - \text{cosine}^2(\bar{\theta}_1, \bar{\theta}_2) \quad (7)$$

We provide in Algorithm 7 the adapted version of the clipped PPO algorithm (Schulman et al., 2017) for learning a subspace of policies. In comparison to the classical approach, the batch of trajectories is first acquired by multiple policies sampled following  $p(z)$  (line 2-3). Then the PPO objective is optimized taking into account the policies used when sampling trajectories (line 4). At last, the critic is updated (line 5), taking as an input the  $z$  value so that it can make robust estimations of the expected reward for all the policies in the subspace. Adapting off-policy algorithms would be similar. Additional details are provided in appendix. Note that, for environments with discrete actions, we have made the same adaptation based on the A2C algorithm since A2C has less hyper-parameters than PPO and is easier to tune, with similar results.

## 4 EXPERIMENTS

We perform experiments in 6 different environments. Implementations based on the *Blind review* library together with train and test environments will be released upon acceptance. For each environment, we consider one train environment on which we trained the different methods, and multiple variations of the training environment for evaluation resulting in 50 test environments in total. The details of all the environment configurations and detailed performance are given in Appendix B. Note that the complete experiments correspond to hundred of trained policies, and dozens of thousands of policy evaluations. For simple control environments (i.e., CartPole, Pendulum and AcroBot), we

<sup>2</sup>Other ways to control the shape of the subspace can be used and we investigate some of them in Section 4

---



---

```

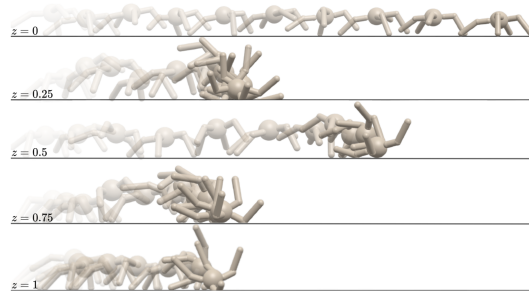
Initialize:  $\bar{\theta}_1, \bar{\theta}_2, \phi$  (Critic),  $n$  batch size
1 for  $k = 0, 1, 2, \dots$  do
2   Sample  $z_1, \dots, z_n \sim \mathcal{U}_{[0,1]}$ 
3   Define  $\theta_{z_i} \leftarrow z_i \bar{\theta}_1 + (1 - z_i) \bar{\theta}_2$ 
4   Sample trajectories  $\{\tau_i\}_1^n$  using  $\{\pi_{\theta_{z_i}}\}$ 
5   Update  $\bar{\theta}_1$  and  $\bar{\theta}_2$  to maximize:
      
$$\frac{1}{n} \sum_{i=1}^n \widehat{\mathcal{L}}_{PPO}(\theta_{z_i}) - \beta \cos^2(\bar{\theta}_1, \bar{\theta}_2)$$

6   Update  $\phi$  to minimize:
      
$$\frac{1}{n} \sum_{i=1}^n \widehat{\mathcal{L}}_{MSE}(\phi, z_i)$$

7 end

```

---



(b) Qualitative example of k-shot adaptation on a modified Ant environment (20% of observations masked). 5 policies are tested on one episode. For  $z = 0.$ , one can see that the Ant is able to adapt to this new environment. More example of LoP trajectories in Figures 4 and 5.

(a) LoP-PPO with  $N = 2$

Figure 2: (Left) The adaptation of the PPO Algorithm with the LoP model. The different with the standard PPO algorithm is that: a) trajectories are sampled using multiple policies  $\theta_{z_i}$  b) The policy loss is augmented with the auxiliary loss, and c) The critic takes the values  $z_i$  as an input. (Right) Examples of trajectories obtained over the Ant with LoP.

introduce few variations of the physics constant at test-time, for instance by varying the mass of the cart, the length of the pole. For complex control environments (i.e., HalfCheetah and Ant using the BRAX library (Freeman et al., 2021), we both use variations of the physics (e.g., gravity), variations of the agent shape (e.g., changing the size of the leg, or of the foot) and sensor alterations. At last, in MiniGrid, we perform experiments where the agent is trained in one particular maze, but is evaluated in other mazes, and particularly in mazes that are bigger than the train maze.

We compare our approach **LoP**<sup>3</sup> with different state-of-the-art methods: a) The **Single** approach is just a single policy learned on the train environment, and evaluated on the test ones. b) The **DIAYN+R**(reward) method is an extension of DIAYN (Eysenbach et al., 2018) where a set of discrete policies is learned using a weighted sum between the DIAYN reward and the task reward:

$$R_{DIAYN+R}(s, a) = r(s, a) + \beta \log p(z|s) \quad (8)$$

Critically, this model requires to choose a discriminator architecture to compute  $\log p(z|s)$  and modifies the train reward by defining an intrinsic reward that may drastically change the behavior of the policies at train time.c) At last, we also compare with the model proposed in (Osa et al., 2021) denoted **Lc** (Latent-conditioned) that works only for continuous actions. This model is also based on a continuous  $z$  variable sampled uniformly at train time, but only uses an auxiliary loss without changing the reward. This auxiliary loss is defined through the joint learning of a density estimation model  $\log P(z|s, a)$  where back-propagation is made over the action  $a$ . As in DIAYN+R, this model needs to carefully define a good neural network architecture for density estimation. Since Lc cannot be used with environment that have discrete actions, we have adapted DIAYN+R (called **DIAYN+R Cont.**) using a continuous  $z$  variable (instead of a discrete one) and a density estimation model  $\log P(z|s)$  as in Osa et al. (2021).

As network architectures, we use multi-layer perceptrons (MLP) with ReLU units for both the policy and the critic (detailed neural network architectures are described in Appendix). For DIAYN+R  $\log P(z|s, \dots)$  is also modeled by a MLP with a soft-max output. For Lc and DIAYN+R Cont.,  $\log P(z|s, \dots)$  is modeled by a MLP that computes the mean of a Gaussian distribution with a fixed variance. For these baselines,  $z$  is concatenated with the environment observation as an input for the policy and the critic models.

<sup>3</sup>We consider the LoP-A2C and the LoP-PPO models for environments with respectively discrete and continuous actions. LoP-PPO could be also used in the discrete case but requires more hyper-parameter tuning.

Nb. Test Env.	CartPole	Acrobot	Pendulum	Minigrid	Brax HalfCheetah	Brax Ant
Type of actions	6 Discr.	6 Discr.	3 Discr.	6 Discr.	16 Cont.	15 Cont.
Single Policy	143.4	-99.7	-52.7	0.169	7697	3338
LoP	149.9	<b>-93.2</b>	<b>-28.9</b>	<b>0.447</b>	<b>10589</b>	<b>4031</b>
DIAYN+R	<b>168.1</b>	-97.0	-47.1	0.248	9680	3759
DIAYN+R $L_2$	156.1	-93.6	-44.0	0.443	-	-
Lc	-	-	-	-	9547	4020

Table 1: Average cumulated reward of the different models over multiple testing environments averaged over 10 training seeds (higher is better). For DIAYN and Lc, we report the results with the best value of  $\beta$  (this is discussed in the main text) and tested 10 policies for LoP, Lc and DIAYN+R using 10 episodes per policy for stochastic environments, and 1 episode per policy on deterministic ones. Standard deviation is reported for each single test environment in Appendix B.

To choose the hyper-parameters of the different methods, let us remind that test environments cannot be used at train time for doing hyper-parameters search and/or model selection which makes this setting particularly difficult. Therefore, we rely on the following procedure: a grid-search over hyper-parameters is made, learning a single policy over the train environment. The best value of the hyper-parameters is then selected as the one that provides the best policy at train time. These hyper-parameters are then used for all the different baselines.

For the adaptation step, each policy is evaluated over 10 episodes for stochastic environments or 1 single episode for deterministic environments. We repeat this procedure over 10 different training seeds, and report the reward over the different test environments together with standard deviation. All detailed results are available in Appendix.

#### 4.1 ANALYSIS

We report the test performance of the models on different environments in Table 1. The table reports the results obtained for the best value of  $\beta$  (multiple values have been tested) which is an optimistic setting where we assume that it is possible to well tune this hyper-parameter. A discussion on that point is made in the next section. In all the environments, the adaptive models perform better than learning a single policy over the train environment which is not surprising. In most of the cases, LoP is able to achieve a better performance than other methods. For instance, on HalfCheetah where we evaluate the different methods over 16 variations of the train environments, LoP achieves an average reward of 10589 while Lc and DIAYN+R obtain respectively 9547 and 9680 (standard deviations are reported in Appendix B). Some examples of the discovered that behaviors in Ant and HalfCheetah<sup>4</sup> for the different methods, and for different values of  $z$  are illustrated in Figures 2b, 4 and 5. This outlines that learning models that are optimal on the train task reward, but with different parameter values, allows us to discover policies react differently to variations of the training environment. It seems to be a better approach than encouraging policies to have a different behaviors (i.e., generating different state distributions) at train time. Same conclusions can be drawn in most of the environments, including MiniGrid where LoP is able to explore large mazes while being trained only on small ones. Interestingly, in CartPole, DIAYN+R performs quite well. Indeed, when analyzing the learned policies, it seems to be a specific case where it is possible to obtain optimal policies that are diverse w.r.t the states they are sampling (by moving the cart more or less on the right/left while maintaining the pole vertical). Said otherwise, CartPole is a setting where the diversity enforced in DIAYN is a good inductive bias that allows the model to discover multiple optimal policies.

We have also performed experiments where test environments have the same dynamics as the training environment, but with defective sensors (i.e., some features at test time have a null value – see Appendix Table B.2 on the Ant environment). The fact that LoP behaves also well confirms the effectiveness of our approach to different types of variations, including noisy features on which baselines methods were not applied in previous publications.

<sup>4</sup>Videos available at <https://sites.google.com/view/subspace-of-policies/home>

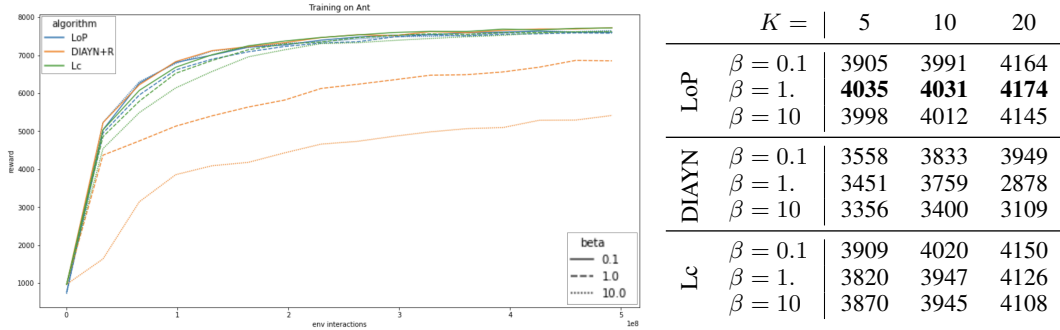


Figure 3: On the left, the evolution of cumulative reward during training on the Ant environment for LoP, DIAYN+R and Lc for different values of  $\beta$ . On the right, the average results obtained by these models on the 15 variations of the train environment. Results are averaged over 10 seeds. Standard error deviation is reported in Table B.2 for each environment.

		SmallFeet	BigFeet	TinyFriction	HugeFriction	SmallGravity	BigGravity
LoP	K=5	8283	<b>8895</b>	<b>10425</b>	<b>11537</b>	<b>11840</b>	<b>10464</b>
	K=10	8805	<b>8903</b>	<b>10662</b>	<b>11659</b>	<b>11969</b>	<b>10578</b>
	K=20	8794	<b>9096</b>	<b>10734</b>	<b>11724</b>	<b>12004</b>	<b>10807</b>
DIAYN+R	K=5	7580	8454	9132	9483	10132	8989
	K=10	7580	8454	9132	9483	10132	8989
	K=20	8255	8472	10003	10335	10568	9766
Lc	K=5	8186	8353	9521	10305	10434	9360
	K=10	8186	8340	9661	10379	10444	9488
	K=20	8107	8431	9661	10505	10521	9506
BoP	K=5	6775	7993	7867	8387	9428	7878
	K=10	6660	8147	7840	8526	9569	8026
	K=20	6996	8405	7963	8553	9666	8015
CoP	K=5	<b>8996</b>	8087	9468	10749	10594	9287
	K=10	<b>9210</b>	8553	9523	10899	11334	9568
	K=20	<b>9155</b>	8754	9979	11047	11382	9695

Table 2: Ablation study on the number of policies  $K$  used at test time on HalfCheetah (see Appendix B.1 for further details and additional results) together with the performance of the BoP and CoP variants. Standard deviation is given in appendix, Table 5.

**Sensitivity to hyper-parameters:** Figure 3 (left) shows the training curves of the different methods, considering different weight values  $\beta$  of the auxiliary loss terms (see Appendix A.3) on Ant<sup>5</sup>. First of all, learning LoP is not slower than learning a single policy, and all the compared methods do not introduce any extra learning cost: we assume that it is due to the sharing of the parameters of the learned policies<sup>6</sup>. It means that LoP can be trained as fast as a single policy. Moreover, DIAYN+R has difficulties to reach a high training performance when the  $\beta$  is high. Indeed, this model introduces an intrinsic reward that prevent the model to be optimal when the  $\beta$  weight is too high. This effect is less visible in Lc and LoP that just use an auxiliary loss, but still visible on Lc whose auxiliary loss tends to modify the behavior of the policies at train time. LoP does not really suffer from high values of  $\beta$  because the method is usually able to satisfy the *cosine* constraint without sacrificing the train reward. In our experiment fixing  $\beta = 1$  always leads to a 0 value for auxiliary term at convergence. As a confirmation, Figure 3 (right) illustrates the test performance of the different methods w.r.t the weight of the auxiliary term. LoP is relatively stable whatever the value of  $\beta$  and  $\beta = 1$  is a good and simple choice. This is a strong point of our method: it does not need any extra hyper-parameter tuning, knowing that such a tuning is impossible when test environments are unknown.

<sup>5</sup>Similar conclusions can be drawn on HalfCheetah and the other environments

<sup>6</sup>In DIAYN, learning one independent policy per value of  $z$  decreases the performance and learning speed.



---

**Online adaptation:** One last interesting property is the number of policies (and thus of episodes) to test over a new environment to get a good performance. For LoP and Lc, given a trained model, one can evaluate as many policies (i.e., different values of  $z$ ) as desired. For DIAYN+R, testing more policies also means training more policies which is expensive and less flexible. Table 2 provides the reward of the different methods when testing  $K$  policies on different HalfCheetah settings: as expected, the performance of DIAYN+R tends to decrease when  $K$  is large since the model has difficulties to learn too many diverse policies. For LoP and Lc, spending more episodes to evaluate more policies naturally leads to a better performance: these two models provide a better way to deal with the exploration-exploitation trade-off at test time. Again, please consider that Lc also needs to define an additional neural network architecture to model  $\log P(z|s, a)$  while LoP does not, making our approach simpler.

**Beyond a Line of Policies:** While LoP is based on the learning of  $N = 2$  anchor parameters, it is possible to combine more than two anchor parameters. We study two approaches combining  $N = 3$  anchor parameters (that can be extended to  $N = 3$ ): a) the first approach is a convex combination of policies (CoP) where  $z$  is sampled following a Dirichlet distribution. (b) The second approach is a Bézier combination (BoP) as explained in Appendix A.2. The results are presented in Table 2 over multiple HalfCheetah environments. It can be seen that these two strategies are not so efficient. LoP is thus a good trade-off between the number of parameters to train and the performance (Note that BoP and CoP need more samples to converge), at least given the particular neural network architectures we have used in this paper.

## 5 RELATED WORK

Our contribution shares connections with different families of approaches. First of all, it focuses on the problem of online adaptation in Reinforcement Learning which has been studied under different terminologies: *Multi-task Reinforcement Learning* (Wilson et al., 2007; Teh et al., 2017), *Transfer Learning* (Taylor and Stone, 2009; Lazaric, 2012) and *Meta-Reinforcement Learning* (Finn et al., 2017; Hausman et al., 2018; Humplik et al., 2019). Many different methods have been proposed, but the best majority considers that the agent is trained over multiple environments such that it can identify variations (or invariant) at train time. For instance, Duan et al. (2016) assume that the agent can sample multiple episodes over the same environments and methods like (Kamienny et al., 2020; Liu et al., 2021) consider that the agent has access to a task identifier at train time.

More recently, diversity-based approaches have been adapted to focus on the setting where only one training environment is available. They share with our model the idea of learning multiple policies instead of a single one. For instance, DIAYN (Eysenbach et al., 2018) learns a discrete set of policies that can be reused and fine-tuned over new environments. It has been adapted to online adaptation in (Kumar et al., 2020a) where the authors propose to combine the intrinsic diversity reward together with the training task reward. This trade-off is obtained through a threshold-based method (instead of a simple weighted sum) with good results. But this method suffers from a major drawback identified in (Osa et al., 2021): it necessitates to sample complete episodes at each epoch which is painful and not adapted to all the RL learning algorithms. Osa et al. (2021) also proposed an alternative based on learning a continuous set of policies instead of a discrete one without using any intrinsic reward.

The method we propose is highly connected to recent researches on mode connectivity with neural networks. Mode connectivity is a set of approaches and analyses that focus on the shape of the parameter space. It has been used as a tool to study generalization in the supervised learning setting (Garipov et al., 2018), but also as a way to propose new algorithms in different settings (Mirzadeh et al., 2021). Obviously, the work that is the most connected to our approach is the model proposed in (Wortsman et al., 2021) that provides a way to learn a subspace of models in the supervised learning setting. Our contribution adapts this approach to RL for learning policies in a completely different setting which is online adaptation.

## 6 CONCLUSION AND PERSPECTIVES

We investigate the idea of learning a subspace of policies in the reinforcement learning setting, and describe how this approach can be used for online adaptation. While simple, our method allows

---

to obtain policies that are robust to variations of the training environments. Contrarily to other techniques, LoP does not need any particular tuning or definition of additional architectures to handle diversity, which is a critical aspect in the online adaptation setting where hyper-parameters tuning is impossible or at least very difficult. Future work includes the extension of this family of approaches in the continual reinforcement learning setting, the deeper understanding of the built subspace and the investigation of different auxiliary losses to better control the shape of such a subspace.

## 7 REPRODUCIBILITY STATEMENT

We have made several efforts to ensure that the results provided in the paper are fully reproducible. In Appendix, we provide a full list of all hyperparameters and extra information needed to reproduce our experiments. More importantly, the source code will be release in the next weeks such that everyone will be able to reproduce the experiments.

## REFERENCES

- G. W. Benton, W. Maddox, S. Lotfi, and A. G. Wilson. Loss surface simplexes for mode connecting volumes and fast ensembling. In M. Meila and T. Zhang, editors, *Proceedings of the 38th International Conference on Machine Learning, ICML 2021, 18-24 July 2021, Virtual Event*, volume 139 of *Proceedings of Machine Learning Research*, pages 769–779. PMLR, 2021. URL <http://proceedings.mlr.press/v139/benton21a.html>.
- G. Brockman, V. Cheung, L. Pettersson, J. Schneider, J. Schulman, J. Tang, and W. Zaremba. Openai gym, 2016.
- M. Chevalier-Boisvert, L. Willems, and S. Pal. Minimalistic gridworld environment for openai gym. <https://github.com/maximecb/gym-minigrid>, 2018.
- Y. Duan, J. Schulman, X. Chen, P. L. Bartlett, I. Sutskever, and P. Abbeel. RI<sup>2</sup>S: Fast reinforcement learning via slow reinforcement learning. *CoRR*, abs/1611.02779, 2016. URL <http://arxiv.org/abs/1611.02779>.
- B. Eysenbach, A. Gupta, J. Ibarz, and S. Levine. Diversity is all you need: Learning skills without a reward function. *CoRR*, abs/1802.06070, 2018. URL <http://arxiv.org/abs/1802.06070>.
- C. Finn, P. Abbeel, and S. Levine. Model-Agnostic Meta-Learning for Fast Adaptation of Deep Networks. *arXiv e-prints*, art. arXiv:1703.03400, Mar 2017.
- C. D. Freeman, E. Frey, A. Raichuk, S. Girgin, I. Mordatch, and O. Bachem. Brax - a differentiable physics engine for large scale rigid body simulation, 2021. URL <http://github.com/google/brax>.
- T. Garipov, P. Izmailov, D. Podoprikin, D. P. Vetrov, and A. G. Wilson. Loss surfaces, mode connectivity, and fast ensembling of dnns. In S. Bengio, H. M. Wallach, H. Larochelle, K. Grauman, N. Cesa-Bianchi, and R. Garnett, editors, *Advances in Neural Information Processing Systems 31: Annual Conference on Neural Information Processing Systems 2018, NeurIPS 2018, December 3-8, 2018, Montréal, Canada*, pages 8803–8812, 2018. URL <https://proceedings.neurips.cc/paper/2018/hash/be3087e74e9100d4bc4c6268cde8456-Abstract.html>.
- K. Hausman, J. T. Springenberg, Z. Wang, N. Heess, and M. A. Riedmiller. Learning an embedding space for transferable robot skills. In *ICLR (Poster)*. OpenReview.net, 2018.
- P. Henderson, W.-D. Chang, F. Shkurti, J. Hansen, D. Meger, and G. Dudek. Benchmark environments for multitask learning in continuous domains. *ICML Lifelong Learning: A Reinforcement Learning Approach Workshop*, 2017.
- J. Humplik, A. Galashov, L. Hasenclever, P. A. Ortega, Y. Whye Teh, and N. Heess. Meta reinforcement learning as task inference. *arXiv e-prints*, art. arXiv:1905.06424, May 2019.

- 
- P. Kamienny, M. Pirota, A. Lazaric, T. Lavril, N. Usunier, and L. Denoyer. Learning adaptive exploration strategies in dynamic environments through informed policy regularization. *CoRR*, abs/2005.02934, 2020. URL <https://arxiv.org/abs/2005.02934>.
- R. Kuditipudi, X. Wang, H. Lee, Y. Zhang, Z. Li, W. Hu, R. Ge, and S. Arora. Explaining landscape connectivity of low-cost solutions for multilayer nets. In H. M. Wallach, H. Larochelle, A. Beygelzimer, F. d’Alché-Buc, E. B. Fox, and R. Garnett, editors, *Advances in Neural Information Processing Systems 32: Annual Conference on Neural Information Processing Systems 2019, NeurIPS 2019, December 8-14, 2019, Vancouver, BC, Canada*, pages 14574–14583, 2019. URL <https://proceedings.neurips.cc/paper/2019/hash/46a4378f835dc8040c8057beb6a2da52-Abstract.html>.
- S. Kumar, A. Kumar, S. Levine, and C. Finn. One solution is not all you need: Few-shot extrapolation via structured maxent RL. In H. Larochelle, M. Ranzato, R. Hadsell, M. Balcan, and H. Lin, editors, *Advances in Neural Information Processing Systems 33: Annual Conference on Neural Information Processing Systems 2020, NeurIPS 2020, December 6-12, 2020, virtual*, 2020a. URL <https://proceedings.neurips.cc/paper/2020/hash/5d151d1059a6281335a10732fc49620e-Abstract.html>.
- S. Kumar, A. Kumar, S. Levine, and C. Finn. One solution is not all you need: Few-shot extrapolation via structured maxent RL. *CoRR*, abs/2010.14484, 2020b. URL <https://arxiv.org/abs/2010.14484>.
- A. Lazaric. Transfer in reinforcement learning: a framework and a survey. In *Reinforcement Learning*, pages 143–173. Springer, 2012.
- E. Z. Liu, A. Raghunathan, P. Liang, and C. Finn. Decoupling exploration and exploitation for meta-reinforcement learning without sacrifices. In M. Meila and T. Zhang, editors, *Proceedings of the 38th International Conference on Machine Learning, ICML 2021, 18-24 July 2021, Virtual Event*, volume 139 of *Proceedings of Machine Learning Research*, pages 6925–6935. PMLR, 2021. URL <http://proceedings.mlr.press/v139/liu21s.html>.
- S. Mirzadeh, M. Farajtabar, D. Görür, R. Pascanu, and H. Ghasemzadeh. Linear mode connectivity in multitask and continual learning. In *9th International Conference on Learning Representations, ICLR 2021, Virtual Event, Austria, May 3-7, 2021*. OpenReview.net, 2021. URL [https://openreview.net/forum?id=Fmg\\_fQYUejf](https://openreview.net/forum?id=Fmg_fQYUejf).
- V. Mnih, A. P. Badia, M. Mirza, A. Graves, T. Harley, T. P. Lillicrap, D. Silver, and K. Kavukcuoglu. Asynchronous methods for deep reinforcement learning. In *Proceedings of the 33rd International Conference on Machine Learning - Volume 48, ICML’16*, page 1928–1937. JMLR.org, 2016.
- T. Osa, V. Tangkaratt, and M. Sugiyama. Discovering diverse solutions in deep reinforcement learning, 2021.
- C. Packer, K. Gao, J. Kos, P. Krähenbühl, V. Koltun, and D. Song. Assessing generalization in deep reinforcement learning, 2018.
- X. B. Peng, M. Andrychowicz, W. Zaremba, and P. Abbeel. Sim-to-Real Transfer of Robotic Control with Dynamics Randomization. *arXiv e-prints*, art. arXiv:1710.06537, Oct 2017.
- J. Schulman, F. Wolski, P. Dhariwal, A. Radford, and O. Klimov. Proximal policy optimization algorithms. *CoRR*, abs/1707.06347, 2017. URL <http://arxiv.org/abs/1707.06347>.
- J. Schulman, P. Moritz, S. Levine, M. Jordan, and P. Abbeel. High-dimensional continuous control using generalized advantage estimation, 2018.
- D. Silver, T. Hubert, J. Schrittwieser, I. Antonoglou, M. Lai, A. Guez, M. Lanctot, L. Sifre, D. Kumaran, T. Graepel, T. P. Lillicrap, K. Simonyan, and D. Hassabis. Mastering chess and shogi by self-play with a general reinforcement learning algorithm. *CoRR*, abs/1712.01815, 2017. URL <http://arxiv.org/abs/1712.01815>.
- M. E. Taylor and P. Stone. Transfer learning for reinforcement learning domains: A survey. *J. Mach. Learn. Res.*, 10:1633–1685, Dec. 2009. ISSN 1532-4435.

- 
- Y. W. Teh, V. Bapst, W. M. Czarnecki, J. Quan, J. Kirkpatrick, R. Hadsell, N. Heess, and R. Pascanu. Distral: Robust multitask reinforcement learning. *CoRR*, abs/1707.04175, 2017. URL <http://arxiv.org/abs/1707.04175>.
- P. N. Ward, A. Smofsky, and A. J. Bose. Improving exploration in soft-actor-critic with normalizing flows policies. *CoRR*, abs/1906.02771, 2019. URL <http://arxiv.org/abs/1906.02771>.
- A. Wilson, A. Fern, S. Ray, and P. Tadepalli. Multi-task reinforcement learning: A hierarchical bayesian approach. In *Proceedings of the 24th International Conference on Machine Learning, ICML '07*, page 1015–1022, New York, NY, USA, 2007. Association for Computing Machinery. ISBN 9781595937933. doi: 10.1145/1273496.1273624. URL <https://doi.org/10.1145/1273496.1273624>.
- M. Wortsman, M. Horton, C. Guestrin, A. Farhadi, and M. Rastegari. Learning neural network subspaces. In M. Meila and T. Zhang, editors, *Proceedings of the 38th International Conference on Machine Learning, ICML 2021, 18-24 July 2021, Virtual Event*, volume 139 of *Proceedings of Machine Learning Research*, pages 11217–11227. PMLR, 2021. URL <http://proceedings.mlr.press/v139/wortsman21a.html>.

---

## A IMPLEMENTATION DETAILS

In this section, we provide details about the implementations of the baselines and our models. Appendix B provides details and additional results for each environment we used.

### A.1 LoP-PPO

We detail the losses used in algorithm 7. First, we recall the clipped-PPO surrogate objective described in Schulman et al. (2017). For a given trajectory  $\tau = \{(s_t, a_t, r_t)\}_0^T$  collected by the policy  $\pi_{\theta_{old}}$ , and denoting  $\rho_t(\theta) = \frac{\pi_{\theta}(a_t|s_t)}{\pi_{\theta_{old}}(a_t|s_t)}$ , the goal is to maximize:

$$\widehat{\mathcal{L}}_{PPO}(\theta) := \frac{1}{T} \sum_{t=0}^T \min[\rho_t(\theta) A^{\pi_{\theta_{old}}}(s_t, a_t), \text{clip}(\rho_t(\theta), 1 + \epsilon, 1 - \epsilon) A^{\pi_{\theta_{old}}}(s_t, a_t)] \quad (9)$$

Where function  $A^{\pi_{\theta_{old}}}$  is computed thanks to a value function  $V_{\phi}$  by using Generalized Advantage Estimation (Schulman et al. (2018)). This function is simultaneously updated by regression on mean-squared error over the rewards-to-go  $\widehat{R}_t$ . In our case, this function not only takes  $s_t$  as an input, but also the value  $z$ :

$$\widehat{\mathcal{L}}_{MSE}(\phi, z) := \frac{1}{T} \sum_{t=0}^T \left( V_{\phi}(s_t, z) - \widehat{R}_t \right)^2 \quad (10)$$

In HalfCheetah and Ant experiments, we sampled actions from a reparametrized Gaussian distribution using a squashing function (Ward et al. (2019)), but we set the standard deviation fixed (so it is an hyper-parameter encouraging exploration, called *action std* in Tables 4 and 7): the policy network only learns the mean of this distribution.

### A.2 BoP AND CoP

The only change between LoP and these models resides in the way we combine the  $N$  anchor policies. For CoP, it is just the generalization of LoP for  $N > 2$  (see 3.1). BoP, makes use of a Bezier parametric curve that uses Bernstein polynomials (the anchor parameters being the *control points*). For  $N = 3$ , it is defined by:

$$\bar{\Theta} = \{(1 - z)^2 \bar{\theta}_1 + 2(1 - z)z \bar{\theta}_2 + z^2 \bar{\theta}_3, \forall z \in [0, 1]\} \quad (11)$$

Concerning the policies  $z$  evaluated at test time, BoP uses the same strategy as LoP by testing values that are uniformly distributed in  $[0, 1]$ . For CoP, we opted for sampling  $K$  policies using a Dirichlet distribution over  $[0, 1]^3$ .

### A.3 DIAYN+R AND LC

In order to find the best trade-off between maximizing environment rewards and intrinsic rewards in DIAYN+R algorithm, we add the hyper-parameter  $\beta$ :

$$R_{DIAYN+R}(s, a) = r(s, a) + \beta \cdot \log p(z|s) \quad (12)$$

As an alternative to DIAYN+R Osa et al. (2021) proposes an algorithm where the discriminator takes not only observations as an input but also the policy output, updating both discriminator  $q_{\phi}$  and policy  $\pi_{\theta}$  when back propagating the gradient. In this case, it is not necessary to add an intrinsic reward. While Osa et al. (2021) illustrate their methods with TD3 and SAC, we adapted it to PPO. The surrogate loss is given by:

$$\mathcal{L}_{LC} := \widehat{\mathcal{L}}_{PPO} + \beta \cdot \log q_{\phi}(z | s, \pi_{\theta}(\cdot | s, z)) \quad (13)$$

---

## B EXPERIMENTS DETAILS AND ADDITIONAL RESULTS

### B.1 HALFCHEETAH

Task originally coming from OpenAI Gym (Brockman et al., 2016). Instead of using MuJoCo engine, we decided to use Brax (Freeman et al., 2021) as it enables the possibility to acquire episodes on GPU. We use the vanilla environment for training. The policy and the critic are encoded by two different multi-layer perceptrons with ReLU activations. The base learning algorithm is PPO.

**Test environments:** we operated modifications similar as the ones proposed in (Henderson et al., 2017). Morphological variations: we changed the radius and mass of specific body parts (torso, thigh, shin, foot). Variations in physics: we changed the gravity and friction coefficients.

Table 3 precisely indicates the nature of the changes for each environment.

Env name	Modifications
BigFeet	Feet mass and radius $\times 1.25$
BigFriction	Friction coefficient $\times 1.25$
BigGravity	Gravity coefficient $\times 1.25$
BigShins	Shins mass and radius $\times 1.25$
BigThighs	Thighs mass and radius $\times 1.25$
BigTorso	Torso mass and radius $\times 1.25$
SmallFeet	Feet mass and radius $\times 0.75$
SmallFriction	Friction coefficient $\times 0.75$
SmallGravity	Gravity coefficient $\times 0.75$
SmallShins	Shins mass and radius $\times 0.75$
SmallThighs	Thighs mass and radius $\times 0.75$
SmallTorso	Torso mass and radius $\times 0.75$
HugeFriction	Friction coefficient $\times 1.5$
HugeGravity	Gravity coefficient $\times 1.5$
TinyFriction	Friction coefficient $\times 0.5$
TinyGravity	Gravity coefficient $\times 0.5$

Table 3: Modified HalfCheetah environments used for testing. Morphological modifications include a variation on the mass and the radius of a specific part of the body (torso, thighs, shins, or feet). We also modified the dynamics (gravity and friction). Environment names are exhaustive: Big refers to a increase of 25% of radius and mass, Small refers to a decrease of 25%. For example, "BigFoot" refers to an HalfCheetah agent where feet have been increased in mass and radius by 25%. For gravity and friction, we also tried an increase/decrease by 50% (respectively tagged "VeryBig" and "VerySmall").

<b>Hyper-parameter</b>	<b>Value</b>
lr policy:	0.0003
lr critic:	0.0003
n parallel environments:	2048
n acquisition steps per epoch:	20
batch size:	512
num minibatches:	32
update epochs:	8
discount factor:	0.99
clip ration:	0.3
action std:	0.5
gae coefficient:	0.96
reward scaling:	1.
gradient clipping:	10.
n layers (policy):	4
n neurons per layer (policy):	64
n layers (critic):	5
n neurons per layer (critic):	256
<b>LoP, BoP, CoP</b>	
$\beta$ :	1
<b>DIAYN</b>	
$\beta$ :	0.1
lr discriminator:	0.0001
n layers (discriminator):	2
n neurons per layer (discriminator):	64
<b>Lc</b>	
$\beta$ :	10
dimensions of z:	1
lr discriminator:	0.001
n layers (discriminator):	2
n neurons per layer (discriminator):	64

Table 4: Hyper-parameters for PPO over HalfCheetah

	Single Policy (K=1)	LoP	DIAYN + R	Lc	BoP	CoP
<b>K=5</b>						
BigFeet	7433 ± 1988	<b>8895 ± 289</b>	8454 ± 655	8353 ± 804	7993 ± 702	8087 ± 496
BigFriction	8579 ± 2224	<b>11635 ± 355</b>	9962 ± 2113	10649 ± 2085	8846 ± 2279	10596 ± 1738
BigGravity	7508 ± 2086	<b>10464 ± 798</b>	8989 ± 1723	9360 ± 1531	7878 ± 1593	9287 ± 1200
BigShins	7274 ± 898	<b>8879 ± 98</b>	8099 ± 806	8206 ± 770	7726 ± 903	8226 ± 1144
BigThig	7963 ± 1466	<b>10054 ± 724</b>	8940 ± 1558	9360 ± 1669	8105 ± 1622	9525 ± 832
BigTorso	7091 ± 2221	<b>9834 ± 310</b>	8701 ± 1472	9198 ± 1342	7790 ± 1713	8927 ± 1128
SmallFeet	5973 ± 2490	8283 ± 648	7580 ± 1411	8186 ± 1512	6775 ± 2308	<b>8996 ± 1150</b>
SmallFriction	8652 ± 1717	<b>11391 ± 348</b>	9813 ± 2074	10181 ± 1617	8652 ± 2075	10459 ± 1387
SmallGravity	9004 ± 1665	<b>11840 ± 406</b>	10132 ± 1903	10434 ± 1951	9428 ± 2180	10594 ± 1438
SmallShin	7492 ± 2999	<b>10840 ± 196</b>	9540 ± 1592	9837 ± 1343	8451 ± 1889	9967 ± 1079
SmallThig	8914 ± 1837	<b>11294 ± 46</b>	10078 ± 1410	10603 ± 1160	9340 ± 1751	10603 ± 1540
SmallTorso	8885 ± 1522	<b>11433 ± 360</b>	9850 ± 1761	10010 ± 1856	9182 ± 1779	10092 ± 1541
HugeFriction	6999 ± 3441	<b>11537 ± 613</b>	9483 ± 2228	10305 ± 2104	8387 ± 2515	10749 ± 1591
HugeGravity	6133 ± 2147	<b>8425 ± 554</b>	7700 ± 1216	7621 ± 1137	6532 ± 1133	7632 ± 903
TinyFriction	7953 ± 1843	<b>10425 ± 211</b>	9132 ± 1862	9521 ± 1462	7867 ± 2003	9468 ± 1468
TinyGravity	7304 ± 3484	<b>11385 ± 169</b>	9363 ± 1734	9620 ± 2041	9118 ± 2360	9020 ± 2028
<b>Average</b>	7697	<b>10413</b>	9114	9465	8254	9514
<b>K=10</b>						
BigFeet	7433 ± 1988	<b>8903 ± 246</b>	8472 ± 535	8340 ± 888	8147 ± 835	8553 ± 1033
BigFriction	8579 ± 2224	<b>11982 ± 330</b>	10781 ± 1870	10705 ± 2092	9093 ± 2436	10850 ± 1526
BigGravity	7508 ± 2086	<b>10578 ± 648</b>	9766 ± 1424	9488 ± 1616	8026 ± 1809	9568 ± 803
BigShins	7274 ± 898	<b>8854 ± 153</b>	8276 ± 607	8340 ± 986	7831 ± 978	8753 ± 866
BigThig	7963 ± 1466	<b>10335 ± 1001</b>	9644 ± 1323	9427 ± 1532	8080 ± 1676	9591 ± 884
BigTorso	7091 ± 2221	<b>10023 ± 427</b>	9295 ± 1106	9271 ± 1317	7928 ± 1772	9131 ± 928
SmallFeet	5973 ± 2490	8805 ± 495	8255 ± 504	8186 ± 1458	6660 ± 1842	<b>9210 ± 1063</b>
SmallFriction	8652 ± 1717	<b>11434 ± 358</b>	10637 ± 1505	10204 ± 1663	8708 ± 2007	10459 ± 1387
SmallGravity	9004 ± 1665	<b>11969 ± 341</b>	10568 ± 1906	10444 ± 1984	9569 ± 2418	11334 ± 1429
SmallShin	7492 ± 2999	<b>10764 ± 147</b>	9990 ± 1107	9933 ± 1315	8441 ± 1801	9898 ± 982
SmallThig	8914 ± 1837	<b>11524 ± 298</b>	10689 ± 1137	10632 ± 1170	9430 ± 1881	10600 ± 1473
SmallTorso	8885 ± 1522	<b>11567 ± 381</b>	10328 ± 1736	10273 ± 1917	9228 ± 1736	10541 ± 1135
HugeFriction	6999 ± 3441	<b>11659 ± 307</b>	10335 ± 1955	10379 ± 2302	8526 ± 2710	10899 ± 1541
HugeGravity	6133 ± 2147	<b>8793 ± 791</b>	8124 ± 1086	7811 ± 1115	6573 ± 1138	8071 ± 352
TinyFriction	7953 ± 1843	<b>10662 ± 385</b>	10003 ± 1226	9661 ± 1497	7840 ± 2019	9523 ± 1537
TinyGravity	7304 ± 3484	<b>11578 ± 460</b>	9723 ± 2167	9650 ± 2228	9221 ± 2224	5107 ± 6910
<b>Average</b>	7697	<b>10589</b>	9680	9547	8331	9506
<b>K=20</b>						
BigFeet	7433 ± 1988	<b>9096 ± 257</b>	8363 ± 800	8431 ± 803	8405 ± 961	8754 ± 1041
BigFriction	8579 ± 2224	<b>12001 ± 276</b>	9655 ± 2304	10779 ± 2158	9108 ± 2437	11124 ± 1397
BigGravity	7508 ± 2086	<b>10807 ± 592</b>	8695 ± 1550	9506 ± 1609	8015 ± 1834	9695 ± 879
BigShins	7274 ± 898	<b>9036 ± 192</b>	7922 ± 670	8393 ± 959	7994 ± 1046	8796 ± 415
BigThig	7963 ± 1466	<b>10521 ± 1016</b>	8639 ± 1315	9537 ± 1633	8159 ± 1602	9652 ± 1012
BigTorso	7091 ± 2221	<b>10084 ± 449</b>	8494 ± 1376	9383 ± 1363	7873 ± 1612	9462 ± 299
SmallFeet	5973 ± 2490	8794 ± 614	7540 ± 1155	8107 ± 1506	6996 ± 2483	<b>9155 ± 497</b>
SmallFriction	8652 ± 1717	<b>11429 ± 319</b>	9603 ± 2022	10271 ± 1680	8844 ± 2162	10498 ± 1331
SmallGravity	9004 ± 1665	<b>12004 ± 259</b>	9934 ± 2370	10521 ± 1986	9666 ± 2280	11382 ± 1377
SmallShin	7492 ± 2999	<b>11041 ± 420</b>	9135 ± 1715	10057 ± 1281	8709 ± 2127	10025 ± 803
SmallThig	8914 ± 1837	<b>11571 ± 127</b>	9970 ± 1847	10682 ± 1092	9563 ± 1820	10921 ± 1018
SmallTorso	8885 ± 1522	<b>11673 ± 434</b>	9620 ± 2009	10315 ± 1880	9301 ± 1814	10602 ± 1297
HugeFriction	6999 ± 3441	<b>11724 ± 685</b>	9438 ± 2471	10505 ± 2355	8553 ± 2603	11047 ± 1167
HugeGravity	6133 ± 2147	<b>8930 ± 714</b>	7498 ± 837	7897 ± 1147	6772 ± 1413	7925 ± 740
TinyFriction	7953 ± 1843	<b>10734 ± 381</b>	9001 ± 1908	9661 ± 1519	7963 ± 2234	9979 ± 878
TinyGravity	7304 ± 3484	<b>11604 ± 388</b>	9419 ± 2317	9822 ± 2200	9329 ± 2424	10822 ± 1045
<b>Average</b>	7697	<b>10691</b>	8933	9617	8453	9990

Table 5: Mean and standard deviation of cumulative reward achieved on HalfCheetah test sets per model (see Table 3 for environment details). Results are averaged over 10 training seeds (i.e., 10 models are trained with the same hyper-parameters and evaluated on the 16 test environments).  $K$  is the number of policies tested at adaptation time, using 1 episode per policy since this environment is deterministic.



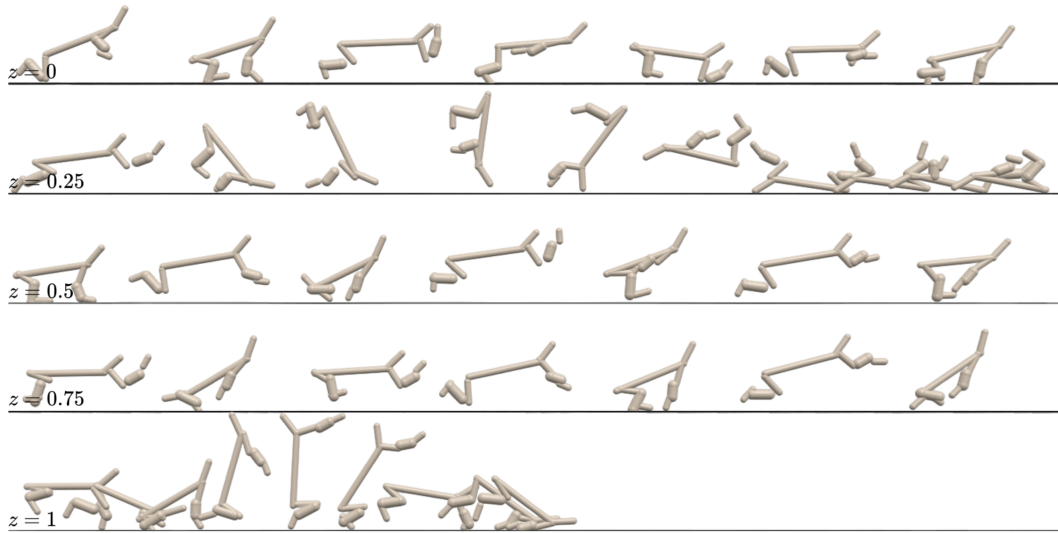


Figure 4: Qualitative example of LoP trajectories on HalfCheetah "BigShins" test environments (5-shot setting). The best reward is obtained for  $z = 0.75$ .

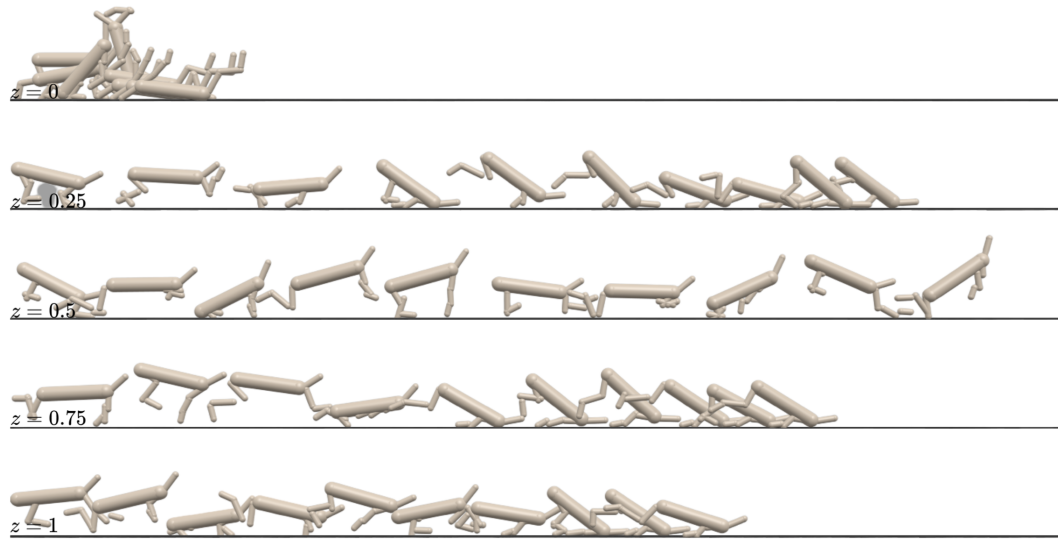


Figure 5: Extreme case: when torso radius and mass are increased by 50%. Only one policy is able to adapt without falling down ( $z = 0.5$ ).

---

## B.2 ANT

Task originally coming from OpenAI Gym (Brockman et al. (2016)). Instead of using MuJoCo engine, we decided to use Brax (Freeman et al. (2021)) as it enables the possibility to acquire episodes on GPU. We use the vanilla environment for training. The policy and the critic are encoded by two different multi-layer perceptrons with ReLU activations. The base learning algorithm is PPO.

**Test environments:** As for HalfCheetah, we operated variations in physics (gravity and friction coefficients). We also designed environments with a percentage of masked features to simulate defective sensors (They are sampled randomly and remain the same for each run). Table 6 precisely indicates the nature of the changes for each environment

Env name	Modifications
BigFriction	Friction coefficient $\times 1.25$
BigGravity	Gravity coefficient $\times 1.25$
SmallFriction	Friction coefficient $\times 0.75$
SmallGravity	Gravity coefficient $\times 0.75$
HugeFriction	Friction coefficient $\times 1.5$
HugeGravity	Gravity coefficient $\times 1.5$
TinyFriction	Friction coefficient $\times 0.5$
TinyGravity	Gravity coefficient $\times 0.5$
DefectiveSensor 5%	5% of env obs set to 0
DefectiveSensor 10%	10% of env obs set to 0
DefectiveSensor 15%	15% of env obs set to 0
DefectiveSensor 20%	20% of env obs set to 0
DefectiveSensor 25%	25% of env obs set to 0
DefectiveSensor 30%	30% of env obs set to 0
DefectiveSensor 35%	35% of env obs set to 0

Table 6: Modified Ant environments used for testing.

<b>Hyper-parameter</b>	<b>Value</b>
lr policy:	0.0003
lr critic:	0.0003
n parallel environments:	2048
n acquisition steps per epoch:	20
batch size:	1024
num minibatches:	16
update epochs:	16
discount factor:	0.99
clip ration:	0.3
action std:	0.4
gae coefficient:	0.96
reward scaling:	1.
gradient clipping:	10.
n layers (policy):	4
n neurons per layer (policy):	64
n layers (critic):	5
n neurons per layer (critic):	256
<b>LoP</b>	
$\beta$ :	{0.1, 1, 10}
<b>DIAYN</b>	
$\beta$ :	{0.1, 1, 10}
lr discriminator:	0.001
n layers (discriminator):	2
n neurons per layer (discriminator):	64
<b>Lc</b>	
$\beta$ :	{0.1, 1, 10}
dimensions of z:	1
lr discriminator:	0.001
n layers (discriminator):	2
n neurons per layer (discriminator):	64

Table 7: Hyper-parameters for PPO over Ant

$\beta =$	Single Policy	LoP			DIAYN + R			Lc		
	(K=1)	0.1	1	10	0.1	1	10	0.1	1	10
<b>K=5</b>										
BigFriction	7454 ± 166	7544 ± 140	7470 ± 96	7541 ± 202	7256 ± 1010	6403 ± 726	6267 ± 627	<b>7666 ± 103</b>	7573 ± 154	7538 ± 136
BigGravity	6905 ± 138	7038 ± 211	6937 ± 23	7027 ± 182	6858 ± 827	6082 ± 583	5865 ± 543	<b>7123 ± 184</b>	7075 ± 168	7051 ± 131
SmallFriction	6755 ± 2073	7695 ± 156	7652 ± 126	7599 ± 167	7046 ± 1777	6491 ± 807	6133 ± 706	<b>7846 ± 127</b>	7673 ± 183	7734 ± 211
SmallGravity	7057 ± 1875	7738 ± 134	7639 ± 120	7748 ± 169	7533 ± 896	6582 ± 727	6486 ± 769	<b>7876 ± 100</b>	7745 ± 105	7772 ± 84
HugeFriction	7505 ± 252	7634 ± 152	7616 ± 68	7601 ± 253	7220 ± 1331	6387 ± 752	6384 ± 733	<b>7799 ± 103</b>	7647 ± 128	7668 ± 77
HugeGravity	380 ± 507	1111 ± 538	1407 ± 557	1494 ± 934	846 ± 556	<b>2924 ± 1992</b>	2847 ± 1598	1134 ± 934	915 ± 465	1440 ± 985
TinyFriction	2747 ± 1241	3716 ± 996	<b>4584 ± 801</b>	4070 ± 1751	3540 ± 948	2950 ± 1113	2600 ± 572	3550 ± 843	4140 ± 294	3487 ± 508
TinyGravity	-520 ± 426	-106 ± 125	-139 ± 274	116 ± 322	-479 ± 374	-3 ± 202	<b>224 ± 108</b>	-234 ± 790	-401 ± 373	-83 ± 329
DefectiveSensor 5%	4308 ± 59	5243 ± 322	<b>5630 ± 124</b>	5560 ± 272	4958 ± 126	4492 ± 211	4360 ± 338	5428 ± 424	4988 ± 123	5225 ± 562
DefectiveSensor 10%	2770 ± 171	3620 ± 238	<b>3660 ± 328</b>	3625 ± 291	3440 ± 64	3371 ± 57	3223 ± 400	3519 ± 76	3406 ± 215	3491 ± 207
DefectiveSensor 15%	1531 ± 90	2583 ± 247	2738 ± 312	<b>2740 ± 167</b>	1774 ± 84	1984 ± 383	2055 ± 311	2408 ± 340	2226 ± 78	2349 ± 271
DefectiveSensor 20%	1026 ± 77	1750 ± 249	1965 ± 234	<b>2008 ± 199</b>	1104 ± 101	1490 ± 387	1450 ± 347	1658 ± 245	1546 ± 108	1714 ± 238
DefectiveSensor 25%	736 ± 95	1595 ± 317	<b>1757 ± 154</b>	1526 ± 338	762 ± 34	1107 ± 396	1120 ± 241	1344 ± 262	1271 ± 205	1363 ± 254
DefectiveSensor 30%	472 ± 50	695 ± 112	793 ± 166	674 ± 120	577 ± 34	<b>859 ± 290</b>	766 ± 212	673 ± 115	575 ± 49	622 ± 100
DefectiveSensor 35%	424 ± 48	606 ± 135	<b>684 ± 182</b>	635 ± 85	449 ± 68	650 ± 245	565 ± 151	618 ± 170	525 ± 92	602 ± 175
<b>Average</b>	3338	3905	<b>4035</b>	3998	3558	3451	3356	3909	3820	3870
<b>K=10</b>										
BigFriction	7454 ± 166	7591 ± 134	7487 ± 101	7556 ± 199	<b>7695 ± 113</b>	6771 ± 573	6021 ± 748	7685 ± 103	7580 ± 163	7554 ± 116
BigGravity	6905 ± 138	7107 ± 153	7015 ± 89	7009 ± 166	<b>7250 ± 57</b>	6282 ± 476	5638 ± 600	7137 ± 96	7083 ± 184	7114 ± 98
SmallFriction	6755 ± 2073	7681 ± 154	7693 ± 103	7671 ± 193	7823 ± 142	6874 ± 590	5980 ± 716	<b>7864 ± 131</b>	7743 ± 161	7762 ± 196
SmallGravity	7057 ± 1875	7788 ± 135	7732 ± 86	7764 ± 185	7886 ± 127	6947 ± 619	6354 ± 818	<b>7896 ± 91</b>	7757 ± 117	7767 ± 75
HugeFriction	7505 ± 252	7640 ± 199	7589 ± 76	7613 ± 238	<b>7860 ± 115</b>	6788 ± 630	6160 ± 767	7846 ± 107	7695 ± 115	7668 ± 79
HugeGravity	380 ± 507	1329 ± 593	1711 ± 74	1583 ± 442	921 ± 302	<b>4564 ± 2033</b>	3009 ± 747	874 ± 358	1237 ± 662	1156 ± 812
TinyFriction	2747 ± 1241	4015 ± 1167	<b>4918 ± 723</b>	4393 ± 1252	4527 ± 560	3001 ± 1261	3676 ± 1382	4545 ± 731	4119 ± 555	3791 ± 476
TinyGravity	-520 ± 426	55 ± 184	11 ± 226	154 ± 293	-56 ± 256	6 ± 236	<b>236 ± 336</b>	-149 ± 800	-248 ± 362	227 ± 357
DefectiveSensor 5%	4308 ± 59	5088 ± 224	5323 ± 173	5098 ± 305	5063 ± 101	4498 ± 191	3992 ± 277	<b>5355 ± 262</b>	5016 ± 109	5229 ± 424
DefectiveSensor 10%	2770 ± 171	3974 ± 380	<b>3978 ± 117</b>	3934 ± 297	3486 ± 161	3413 ± 213	3061 ± 184	3960 ± 106	3711 ± 194	3779 ± 196
DefectiveSensor 15%	1531 ± 90	<b>2504 ± 283</b>	2423 ± 154	2496 ± 92	1851 ± 142	2365 ± 426	2226 ± 216	2309 ± 137	2374 ± 120	2352 ± 127
DefectiveSensor 20%	1026 ± 77	1795 ± 174	1629 ± 111	1774 ± 147	1205 ± 63	1777 ± 466	1737 ± 203	1834 ± 326	<b>1987 ± 127</b>	1787 ± 180
DefectiveSensor 25%	736 ± 95	<b>1486 ± 156</b>	1351 ± 220	1372 ± 85	851 ± 36	1422 ± 411	1380 ± 218	1342 ± 121	1368 ± 95	1390 ± 93
DefectiveSensor 30%	472 ± 50	1103 ± 87	968 ± 93	<b>1133 ± 158</b>	635 ± 99	967 ± 297	866 ± 157	1069 ± 144	925 ± 109	962 ± 149
DefectiveSensor 35%	424 ± 48	<b>714 ± 149</b>	640 ± 86	634 ± 75	441 ± 49	<b>714 ± 223</b>	662 ± 109	583 ± 95	609 ± 122	630 ± 107
<b>Average</b>	3338	3991	<b>4031</b>	4012	3833	3759	3400	4020	3947	3945
<b>K=20</b>										
BigFriction	7454 ± 166	7592 ± 147	7510 ± 89	7569 ± 172	7646 ± 118	4328 ± 3086	5301 ± 429	<b>7692 ± 94</b>	7589 ± 129	7573 ± 122
BigGravity	6905 ± 138	7121 ± 162	7028 ± 50	7090 ± 171	<b>7196 ± 139</b>	4172 ± 2949	4867 ± 370	7162 ± 86	7135 ± 147	7132 ± 121
SmallFriction	6755 ± 2073	7767 ± 111	7712 ± 98	7703 ± 228	7833 ± 141	4360 ± 3118	5021 ± 322	<b>7862 ± 131</b>	7726 ± 144	7775 ± 170
SmallGravity	7057 ± 1875	7807 ± 123	7698 ± 86	7777 ± 203	7863 ± 109	4512 ± 3258	5343 ± 404	<b>7906 ± 78</b>	7774 ± 113	7806 ± 95
HugeFriction	7505 ± 252	7674 ± 171	7648 ± 97	7699 ± 198	7747 ± 104	4331 ± 3089	5061 ± 334	<b>7851 ± 119</b>	7714 ± 115	7737 ± 81
HugeGravity	380 ± 507	1655 ± 712	2111 ± 1405	1587 ± 343	2005 ± 743	3596 ± 2437	<b>4231 ± 121</b>	1357 ± 197	2122 ± 1006	1514 ± 845
TinyFriction	2747 ± 1241	4437 ± 827	<b>5147 ± 595</b>	4625 ± 1145	4393 ± 469	2203 ± 1432	3117 ± 816	4707 ± 490	3979 ± 656	3917 ± 529
TinyGravity	-520 ± 426	259 ± 324	188 ± 241	289 ± 316	<b>357 ± 525</b>	291 ± 620	348 ± 152	-121 ± 812	-110 ± 257	177 ± 370
DefectiveSensor 5%	4308 ± 59	5816 ± 313	5996 ± 153	6002 ± 216	5185 ± 121	4570 ± 175	3647 ± 174	<b>6023 ± 257</b>	5780 ± 241	5884 ± 177
DefectiveSensor 10%	2770 ± 171	3979 ± 248	3850 ± 199	4083 ± 313	3500 ± 208	3475 ± 242	2827 ± 261	<b>4173 ± 325</b>	4023 ± 176	4038 ± 391
DefectiveSensor 15%	1531 ± 90	2789 ± 368	2526 ± 132	2790 ± 367	2047 ± 117	2495 ± 52	2125 ± 218	2596 ± 306	<b>3011 ± 202</b>	2810 ± 403
DefectiveSensor 20%	1026 ± 77	1890 ± 107	1794 ± 88	1750 ± 278	1333 ± 86	1875 ± 26	1714 ± 189	1746 ± 123	1789 ± 151	<b>1901 ± 185</b>
DefectiveSensor 25%	736 ± 95	<b>1582 ± 104</b>	1422 ± 187	1416 ± 150	992 ± 51	1351 ± 16	1320 ± 217	1480 ± 128	1286 ± 166	1450 ± 195
DefectiveSensor 30%	472 ± 50	<b>1102 ± 133</b>	1069 ± 128	968 ± 62	657 ± 75	931 ± 136	994 ± 70	909 ± 178	1035 ± 99	992 ± 51
DefectiveSensor 35%	424 ± 48	<b>996 ± 103</b>	908 ± 104	833 ± 77	485 ± 67	678 ± 15	719 ± 59	791 ± 100	927 ± 92	907 ± 113
<b>Average</b>	3338	4164	<b>4174</b>	4145	3949	2878	3109	4150	4126	4108

Table 8: Mean and standard deviation of cumulative reward achieved on Ant test sets per model. Results are averaged over 10 training seeds (i.e., 10 models are trained with the same hyper-parameters and evaluated on the 12 test sets).  $K$  is the number of policies tested at adaptation time, using 1 episode per policy since this environment is deterministic. For this environment, we split the results per  $\beta$  value as it has been used for beta ablation study (see Figure 3)

### B.3 CARTPOLE

We use the openAI gym implementation of CartPole as a training environment. The 6 test environments are provided by Packer et al. (2018) where three different factors may vary: the mass of the cart, the length of the pole and the force applied to the cart. The length of each episode is 200. The policy and the critic are encoded by two different multi-layer perceptrons with ReLU activations. The base learning algorithm is A2C.

Environment	Characteristics
(Train) CartPole	$mass = 0.1, length = 0.5, force = 10.0$
HeavyPole CartPole	$mass = 1.0$
LightPole CartPole	$mass = 0.001$
LongPole CartPole	$length = 1.0$
ShortPole CartPole	$length = 0.05$
StrongPush CartPole	$force = 20.0$
WeakPush CartPole	$force = 1.0$

Table 9: CartPole train and test environments

Hyper-parameter	Value
learning rate:	0.001
n acquisition steps per epoch:	8
n parallel environments:	32
critic coefficient:	1.0
entropy coefficient:	0.001
discount factor:	0.99
gae coefficient:	1.0
gradient clipping:	2.0
n neurons per layer:	8
n layers:	2
LoP	
$\beta$ :	1.0
DIAYN	
$\beta$ :	1.0
n neurons per layer discriminator:	8
n layers discriminator:	2
learning rate discriminator:	0.001

Table 10: Hyper-parameters for A2C over CartPole

	Single	LoP	DIAYN+R	DIAYN+R $L_2$
HeavyPole CartPole	200.0 $\pm$ 0.0	200.0 $\pm$ 0.0	200.0 $\pm$ 0.0	200.0 $\pm$ 0.0
LightPole CartPole	200.0 $\pm$ 0.0	200.0 $\pm$ 0.0	200.0 $\pm$ 0.0	200.0 $\pm$ 0.0
LongPole CartPole	54.4 $\pm$ 81.6	56.1 $\pm$ 72.2	163.3 $\pm$ 73.3	123.8 $\pm$ 86.2
ShortPole CartPole	67.0 $\pm$ 33.1	78.9 $\pm$ 25.3	50.7 $\pm$ 18.1	64.8 $\pm$ 31.2
StrongPush CartPole	200.0 $\pm$ 0.0	200.0 $\pm$ 0.0	200.0 $\pm$ 0.0	199.9 $\pm$ 0.2
WeakPush CartPole	138.9 $\pm$ 43.8	164.4 $\pm$ 18.3	194.3 $\pm$ 10.0	148.1 $\pm$ 64.8
Average	143.4	149.9	<b>168.1</b>	156.1

Table 11: Results over CartPole, using 10 policies, and 10 episodes per policy at adaptation time.

## B.4 ACROBOT

We use the openAI gym implementation of Acrobot as a training environment. The 4 test environments are provided by Packer et al. (2018) where two different factor may vary: the inertia factor and the length of the system. We have used A2C as a learning algorithm.

Environment	Characteristics
(Train) Acrobot	$mass = 0.1, length = 1.0, inertia = 1.0$
Heavy Acrobot	$mass = 1.5$
HighInertia Acrobot	$inertia = 1.5$
Light Acrobot	$mass = 0.5$
Long Acrobot	$length = 1.5$
LowInertia Acrobot	$inertia = 0.5$
Short Acrobot	$length = 0.5$

Table 12: Acrobot train and test environments

Hyper-parameter	Value
learning rate:	0.001
n acquisition steps per epoch:	8
n parallel environments:	32
critic coefficient:	1.0
entropy coefficient:	0.001
discount factor:	0.99
gae coefficient:	0.7
gradient clipping:	2.0
n neurons per layer:	16
n layers:	2
LoP	
$\beta$ :	1.0
DIAYN	
$\beta$ :	1.0
n neurons per layer discriminator:	16
n layers discriminator:	2
learning rate discriminator:	0.001

Table 13: Hyper-parameters for A2C over Acrobot

	Single	LoP	DIAYN+R	DIAYN+R $L_2$
Heavy Acrobot	$-108.4 \pm 3.2$	$-105.1 \pm 1.0$	$-108.0 \pm 1.8$	$-108.2 \pm 4.4$
HighInertia Acrobot	$-108.7 \pm 5.6$	$-99.8 \pm 2.8$	$-106.0 \pm 2.7$	$-106.8 \pm 8.9$
Light Acrobot	$-120.7 \pm 71.3$	$-107.2 \pm 58.8$	$-115.2 \pm 33.1$	$-93.1 \pm 37.3$
Long Acrobot	$-124.3 \pm 2.7$	$-115.8 \pm 9.6$	$-117.3 \pm 4.1$	$-117.5 \pm 5.3$
LowInertia Acrobot	$-71.3 \pm 2.3$	$-70.7 \pm 0.7$	$-71.2 \pm 0.7$	$-71.3 \pm 1.9$
Short Acrobot	$-65.1 \pm 2.8$	$-60.7 \pm 0.6$	$-64.2 \pm 2.6$	$-64.7 \pm 5.6$
Average	-99.7	<b>-93.2</b>	-97.0	-93.6

Table 14: Results over Acrobot, using 10 policies, and 10 episodes per policy at adaptation time.

## B.5 PENDULUM

We use the openAI gym implementation of Pendulum as a training environment. The 3 test environments are provided by Packer et al. (2018) where two different factor may vary: the mass and the length of the pendulum. We have considered 5 discrete actions between  $-1$  and  $+1$ . We have used A2C as a learning algorithm.

Environment	Characteristics
(Train) Pendulum	$mass = 1.0, length = 1.0$
Light Pendulum	$mass = 0.5$
Long Pendulum	$length = 1.5$
Short Pendulum	$length = 0.5$

Table 15: Pendulum train and test environments

Hyper-parameter	Value
learning rate:	0.001
n acquisition steps per epoch:	8
n parallel environments:	32
critic coefficient:	1.0
entropy coefficient:	0.001
discount factor:	0.99
gae coefficient:	0.7
gradient clipping:	2.0
n neurons per layer:	16
n layers:	2
<b>LoP</b>	
$\beta$ :	1.0
<b>DIAYN</b>	
$\beta$ :	1.0
n neurons per layer discriminator:	16
n layers discriminator:	2
learning rate discriminator:	0.001

Table 16: Hyper-parameters for A2C over Pendulum

	Single	LoP	DIAYN+R	DIAYN+R $L_2$
Light Pendulum	$-36.5 \pm 58.5$	$-11.4 \pm 2.7$	$-39.3 \pm 10.9$	$-32.1 \pm 15.4$
Long Pendulum	$-82.1 \pm 20.4$	$-64.5 \pm 13.0$	$-70.6 \pm 15.2$	$-71.9 \pm 17.3$
Short Pendulum	$-39.6 \pm 66.9$	$-10.7 \pm 2.1$	$-31.3 \pm 11.7$	$-28.2 \pm 13.3$
Average	$-52.7$	<b><math>-28.9</math></b>	$-47.1$	$-44.0$

Table 17: Results over Pendulum, using 10 policies, and 10 episodes per policy at adaptation time.

## B.6 MINIGRID

We have use Gym Minigrd to perform experiments on mazes Chevalier-Boisvert et al. (2018). We have used the MultiRoom-N2-S4 for training considering one single maze. At test time, we have tested on three different MultiRoom-N2-S4 environments composed of two rooms, but also on three MultiRoom-N4-S5 composed of four rooms. This allows us to evaluate the generalization power of the different methods to larger mazes. We have used A2C as a learning algorithm.

Hyper-parameter	Value
learning rate:	0.001
n acquisition steps per epoch:	8
n parallel environments:	32
critic coefficient:	1.0
entropy coefficient:	0.001
discount factor:	0.99
gae coefficient:	0.7
gradient clipping:	2.0
n neurons per layer:	16
n layers:	2
LoP	
$\beta$ :	1.0
DIAYN	
$\beta$ :	1.0
n neurons per layer discriminator:	16
n layers discriminator:	2
learning rate discriminator:	0.001

Table 18: Hyper-parameters for A2C over Minigrd

	Single	LoP	DIAYN+R	DIAYN+R $L_2$
Two Rooms Maze 1	$0.387 \pm 0.447$	$0.619 \pm 0.309$	$0.348 \pm 0.348$	$0.656 \pm 0.328$
Two Rooms Maze 2	$0.433 \pm 0.499$	$0.865 \pm 0.0$	$0.627 \pm 0.363$	$0.692 \pm 0.346$
Two Rooms Maze 3	$0.194 \pm 0.387$	$0.617 \pm 0.309$	$0.348 \pm 0.353$	$0.656 \pm 0.328$
Four Rooms Maze 1	$0.0 \pm 0.0$	$0.294 \pm 0.36$	$0.0 \pm 0.0$	$0.24 \pm 0.359$
Four Rooms Maze 2	$0.0 \pm 0.0$	$0.004 \pm 0.007$	$0.0 \pm 0.0$	$0.137 \pm 0.274$
Four Rooms Maze 3	$0.0 \pm 0.0$	$0.281 \pm 0.345$	$0.166 \pm 0.287$	$0.28 \pm 0.345$
Average	0.169	<b>0.447</b>	0.248	0.443

Table 19: Results over Minigrd, using 10 policies, and 1 episode per policy at adaptation time.